Available online at www.sciencedirect.com
SciVerse ScienceDirect
Journal of Genetics and Genomics 39 (2012) 93−102
JGG

ORIGINAL RESEARCH

Identification of a Ubiquitin-Binding Structure in the S-Locus F-Box Protein Controlling S-RNase-Based Self-Incompatibility

Guang Chen [a,b,c,1], Bin Zhang [a,b,c,1], Lijing Liu [b,c], Qun Li [a], Yu'e Zhang [a], Qi Xie [b], Yongbiao Xue [a,*]

[a] *State Key Laboratory of Molecular Developmental Biology, Institute of Genetics and Developmental Biology, Chinese Academy of Sciences and National Center for Plant Gene Research, Beijing 100101, China*
[b] *State Key Laboratory of Plant Genomics, Institute of Genetics and Developmental Biology, Chinese Academy of Sciences and National Center for Plant Gene Research, Beijing 100101, China*
[c] *Graduate University of Chinese Academy of Sciences, Beijing 100190, China*

Received 31 December 2011; accepted 6 January 2012
Available online 14 January 2012

ABSTRACT

In flowering plants, self-incompatibility (SI) serves as an important intraspecific reproductive barrier to promote outbreeding. In species from the Solanaceae, Plantaginaceae and Rosaceae, S-RNase and SLF (S-locus F-box) proteins have been shown to control the female and male specificity of SI, respectively. However, little is known about structure features of the SLF protein apart from its conserved F-box domain. Here we show that the SLF C-terminal region possesses a novel ubiquitin-binding domain (UBD) structure conserved among the SLF protein family. By using an *ex vivo* system of *Nicotiana benthamiana*, we found that the UBD mediates the SLF protein turnover by the ubiquitin−proteasome pathway. Furthermore, we detected that the SLF protein was directly involved in S-RNase degradation. Taken together, our results provide a novel insight into the SLF structure and highlight a potential role of SLF protein stability and degradation in S-RNase-based self-incompatibility.

KEYWORDS: Protein degradation; SLF; Ubiquitin; Self-incompatibility; Ubiquitin-binding structure; S-RNase

1. INTRODUCTION

The F-box motif-containing proteins are found throughout eukaryotes as key regulators of diverse biological pathways. They are mainly required for protein ubiquitination and degradation process, which generally employs an E1 (ubiquitin activating enzyme)-E2 (ubiquitin conjugating enzyme)-E3 (ubiquitin ligase) cascade for covalent addition of a ubiquitin chain to a substrate (Petroski and Deshaies, 2005; Vierstra, 2009). In most cases, an F-box protein contributes the formation of an SCF (SKP1/Cullin/F-box) E3 ligase complex and contains two major domains, an F-box motif interacting with the SKP1 protein and a protein−protein interaction domain serving as a substrate recognition domain (Schulman et al., 2000; Hua and Vierstra, 2011).

Plants contain the largest known number of F-box proteins in eukaryotes. In *Arabidopsis*, at least 700 F-box proteins have been annotated and some of them are found to act as essential regulators during its development and signaling transduction process (Gagne et al., 2002). For example, the receptors of phytohormones auxin and jasmonic acid have been demonstrated to be F-box proteins TIR1 and COI1, respectively (Xie et al., 1998; Dharmasiri et al., 2005; Kepinski and Leyser, 2005; Yan et al., 2009), with their protein−protein interaction

Abbreviations: SLF, S-locus F-box; S-RNase, S-Ribonucleases; UBD, ubiquitin-binding domain; UPS, ubiquitin−proteasome system; SI, self-incompatibility; CPC, cross-pollen compatibility; SPI, self-pollen incompatibility; SSK1, SLF-interacting SKP1-like 1; CTD, C-terminal domainSCF, SKP1/Cullin1/F-box; LRR, leucine-rich repeats; GFP, green fluorescent protein.

* Corresponding author. Tel: +86 10 6255 2880, fax: +86 10 6253 7814.
E-mail address: ybxue@genetics.ac.cn (Y. Xue).

[1] These authors contributed equally to this work.

doi:10.1016/j.jgg.2012.01.001

domains defined as leucine-rich repeats (LRR) (Patton et al., 1998; Finn et al., 2008). Besides, other protein−protein interaction domains of the F-box proteins have also been found, such as Kelch- and WD40-repeats domain (Patton et al., 1998; Finn et al., 2008). However, there are still numerous types of F-box proteins with unknown protein−protein interaction domains, like CEGENDUO involved in auxin-mediated lateral root formation (Dong et al., 2006) and DOR involved in ABA-induced stomatal closure under drought stress (Zhang et al., 2008). In addition, recent findings have revealed that the protein−protein interaction domains of the F-box proteins often exhibit a ubiquitin binding property and some of them have been defined as novel ubiquitin-binding domains (UBD) (Pashkova et al., 2010). For example, the WD40-repeats form a β-propeller structure and bind ubiquitin, providing an alternative function of the protein−protein interaction domains (Pashkova et al., 2010).

Plant self-incompatibility (SI) is an intraspecific genetic barrier to distinguish self (genetic-related) and non-self (genetic-unrelated) pollen and reject self one (de Nettancourt, 2001; Franklin-Tong, 2008). Genetic studies show that the multiallelic genes encoded by the *S*-locus determine male (pollen-part) and female (pistil-part) specificity of SI, respectively (Takayama and Isogai, 2005; Zhang et al., 2009). Molecular analysis reveals that many species in Solanaceae, Plantaginaceae and Rosaceae employ S-RNase (S-ribonuclease) as the pistil specificity determinant and SLF (S-locus F-box) for the pollen part (Lee et al., 1994; Murfett et al., 1994; Lai et al., 2002; Sijacic et al., 2004; Qiao et al., 2004b). In this self-incompatibility system, S-RNases are extracellular proteins thought to be cytotoxic to the pollen tube growth (McClure et al., 1990) whereas the SLF protein family has been found to be clustered into at least six types and three of them are shown to act together for a collaborative recognition of non-self S-RNases (Kubo et al., 2010). The SLF represents a highly-conserved F-box protein family with a protein−protein interaction domain (C-terminal domain, CTD), by which it interacts with S-RNases (Qiao et al., 2004a; Hua et al., 2007). Recently, the interaction affinity analysis between S-RNase and SLF has shown that a non-self pair appears to display a stronger affinity than a self one, indicating that the CTD contains a potential structural specificity discriminating self/non-self pollen (Hua et al., 2007). In addition, SSK1 (SLF-interacting SKP1-like 1) proteins have been shown to be a novel class of pollen-specific SKP1-like proteins that bridge Cullin1 and SLF proteins to form an SCF complex in *Antirrhinum hispanicum* (Plantaginaceae) and *Petunia hybrida* (Solanaceae) (Huang et al., 2006; Zhao et al., 2010). On the basis of these findings, a protein degradation model has been proposed that non-self S-RNases are specifically targeted by the SCF^{SLF} E3 ligase complex to the ubiquitin−proteasome system (UPS) for degradation, thus allowing non-self pollen tube to grow (cross-pollen compatibility, CPC); whereas self S-RNases somehow remain active and thus are cytotoxic to pollen tube growth (self-pollen incompatibility, SPI) (Lai et al., 2002; Kao and Tsukamoto, 2004; Hua et al., 2008; Zhang and Xue, 2008; Chen et al., 2010a).

As is known, a canonical function of F-box proteins is to modulate the substrate protein stability by mediating its ubiquitination and subsequent degradation through the ubiquitin−proteasome system. Nevertheless, recent studies have indicated that F-box proteins themselves also are regulated by the proteasome-mediated proteolysis in mammals, yeast and plants (Zhou and Howley, 1998; Galan and Peter, 1999; Mathias et al., 1999; Wirbelauer et al., 2000; Li et al., 2004; Kim et al., 2007; van den Burg et al., 2008; Stuttmann et al., 2009; An et al., 2010; Nibau et al., 2011). Interestingly, several F-box proteins have been reported to contain a ubiquitin-binding domain to interact with ubiquitin or ubiquitin chains leading to its own degradation by the proteasome (Pashkova et al., 2010).

Apart from the F-box motif, little is known about the structure and function of the CTD of SLF proteins. Here we show that the SLF CTD contains a novel and conserved ubiquitin-binding domain. It was found to be similar to that in many F-box proteins in plants, yeast and mammals at a three dimensional structural level. We employed an *ex vivo* system in *Nicotiana benthamiana* to investigate biochemical relationships among SLF, S-RNase and SSK1 proteins and found that the SLF protein could regulate the stability of S-RNase protein. Interestingly, we demonstrated that the protein stability of SLF proteins themselves could be modulated through the ubiquitin−proteasome pathway. Our results provided a novel insight into the SLF structure and revealed a potential role of its turnover in S-RNase-based self-incompatibility.

2. MATERIALS AND METHODS

2.1. Plant growth and agroinfiltration procedure

Wild-type *N. benthamiana* plants were grown at 22°C and 70% relative humidity under 16 h/8 h light/dark condition for 1 month before agroinfiltration. The infiltrated plants were grown under the same conditions. The agroinfiltration procedure was performed accordingly with several modifications as follows (Liu et al., 2010). *Agrobacterium tumefaciens* strain EHA105 was transformed with binary constructs as indicated in the study and plated on YEB medium for antibiotic selection. A single colony was inoculated into 5 mL YEB medium with appropriate antibiotics and grown at 28°C for 48 h and transferred to a new YEB medium containing 10 mmol/L 2-(*N*-morpholine)-ethanesulfonic acid (MES, pH 5.6) and 40 μmol/L acetosyringone. Bacteria were cultured at 28°C until the OD_{600} reached 3.0 and then centrifuged at 3200 *g* for 10 min before the pellets were resuspended in 10 mmol/L $MgCl_2$ to adjust the OD_{600} to 1.5 ($OD_{600} = 1$ for p19 strain). Acetosyringone was added at a final concentration of 200 μmol/L and the culture was kept at least 3 h without shaking at room temperature. Leaf infiltration was performed by depressing a 1-mL disposable syringe to the surface of fully expanded leaves. For co-infiltrations, equal volume of suspension culture was mixed before infiltration. The p19 factor was mixed with other plasmid-containing *Agrobacterium* except that in the test of its influence on protein expression. The proteasome inhibitor MG132 was infiltrated as indicated.

2.2. Binary constructs

Previously cloned *PhS$_{3L}$RNase*, *PhSLF-S$_1$*, *PhSSK1* and *PhSLF-S$_{3L}$* (Qiao et al., 2004a, 2004b; Zhao et al., 2010) were used as templates for PCR amplification of the corresponding gene fragment for generating binary constructs used in this study (Table S1). The pCAMBIA-1300-221 and pBA002-Myc vectors were constructed previously (Liu et al., 2010). *PhS$_{3L}$RNase* and *PhSSK1* fragments were inserted into pCAMBIA-1300-221 *via* a *Kpn* I digest, respectively. *PhSLF-S$_1$* and *PhSSK1* fragments were inserted into pBA002-Myc *via* an *Xma* I/*Spe* I digest, respectively. For yeast two-hybrid assay, *PhSLF-S$_1$* and *PhSLF-S$_{3L}$* C-terminal fragments were inserted into *pGBKT7* (CLONTECH, USA) as described previously (Huang et al., 2006; Zhao et al., 2010); whereas *P. hybrida ubiquitin* and *ubiquitin*^{L8AR42EI44A} fragments were cloned into *pGADT7* (CLONTECH) through *Eco*R I/*Xho* I digest, respectively. The primers used in this study were listed in Table S1.

2.3. Quantification analysis by yeast two-hybrid assay

PhSLF-S$_1$ and *PhSLF-S$_{3L}$* C-terminal cDNA and full-length cDNA of *P. hybrida ubiquitin* and *ubiquitin*^{L8AR42EI44A} were ligated into *pGBKT7* and *pGADT7* (CLONTECH) to produce in-frame GAL4 BD as baits and GAL4 AD as preys fusions, respectively. The constructs were co-transformed into yeast strain AH109 for interaction assay. The yeast culture was plated onto synthetic drop out (SD) medium lacking leucine and tryptophan to test for co-transformation. After the grow test on SD/-Trp-Leu-His-Ade, the corresponding yeast grown on the medium lacking leucine and tryptophan was used for quantification of the interaction affinity as follows. An overnight culture was transferred to YPD medium and incubated at 30°C for 3 h with shaking (250 r/min). Exact OD_{600} value was recorded before harvest the cells. The resuspended cells by Z-buffer were frozen in liquid nitrogen. After a 37°C water bath for 1 min, Z-buffer with ONPG (*O*-Nirophenyl-β-D-Galactopyranoside), the substrate of β-galactosidase, was added and started timing immediately. When the yellow color developed, 1 mol/L Na_2CO_3 was added to the reaction and blank tubes. After an elapsed time, the reaction tubes were centrifuged for 10 min at 14,000 r/min. After calibration of the spectrophotometer against the blank at A_{420} and measuring the OD_{420} of the samples, β-galactosidase units were calculated as follows. β-galactosidase units $= 1000 \times OD_{420}/(t \times V \times OD_{600})$, where t indicated elapsed time of incubation (in min), V 0.1 mL × concentration factor, and OD_{600} A_{600} of 1 mL of culture. One unit of β-galactosidase equaled the amount which hydrolyzes 1 μmol of ONPG per min per cell.

2.4. Protein structure modeling

P. hybrida SLF proteins were modeled using the iTasser server (http://zhanglab.ccmb.med.umich.edu/I-TASSER/) (Roy et al., 2010). iTasser provides a robust meta-threading alignment for identification of template structures and generates a final model after iterative simulations. In our study, iTasser predicted the secondary structure of PhSLF and its solvent accessibility, and finally identified template structures 2OVR, 2ZWA, 2OVP, 1QFM and 3FW0, providing five ranked models. iTasser recognized 2OVR chain B (human Fbw7) as a closest structural homolog in the five ranked models. The quality of the predicted models was assessed by QMEAN server (Benkert et al., 2008) and confirmed its confidence degree by MOLPROBITY (Chen et al., 2010b). The structure comparison was performed by submitting the PhSLF-CTD to the Dali server (http://ekhidna.biocenter.helsinki.fi/dali_server/) (Holm and Rosenstrom, 2010). Protein structural similarity was identified and WD-repeats domains were found to be close to the PhSLF-CTD with a Z-score at 10.5. Similarity with a Z-score lower than 2 was spurious. Each neighbour had links to a pairwise structural alignment with the query structure, to precomputed structural neighbours in the Dali Database, and to the PDB format coordinate file where the neighbour was superimposed onto the query structure. The SLF−SSK1 interface structure was obtained through ICM-Chemist-Pro (http://www.molsoft.com/chemistpro/index.html), based on the ICM ODA (optimal docking areas) theory. All the structural images were produced by using the PyMol molecular visualization package (http://www.pymol.org).

2.5. RT-PCR amplification

To detect the gene expression level by RT-PCR, approximately 2 μg total RNA was extracted (TRIzol) to a reverse transcription reaction at 42°C for 1 h. The following PCR amplification reaction was performed by using gene-specific forward and reverse primers for 28 cycles (Table S1). Expression level of *Actin* of *N. benthamiana* (short for *ACT1*) was used as an internal control in this study.

2.6. Protein extraction and immunoprecipitation

Infiltrated parts of *N. benthamiana* leaves were harvested and ground in liquid nitrogen before resuspended in extraction buffer (50 mmol/L Tris-MES, pH 8.0, 0.5 mol/L sucrose, 1 mmol/L $MgCl_2$, 10 mmol/L EDTA, 5 mmol/L DTT, protease inhibitor cocktail CompleteMini tablets, ROCHE, USA) on ice. The total extracts were centrifuged at 16,000 *g* for 30 min at 4°C, and the supernatant was subjected to protein immunoblots. For protein immunoprecipitation analysis, antibodies were added as indicated at a final concentration of 10 μg/mL and MG132 (50 μmol/L) (SIGMA, USA) was also added into the cell lysates to inhibit protein degradation. The mixture was kept for 3 h at 4°C with a gentle shaking. After that 20 μL/mL protein G agarose beads (16-266 MILLIPORE, USA) were added and continued shaking for another 3 h at 4°C. At last the immunocomplex was purified and subjected to protein immunoblots.

2.7. Protein immunoblot

Protein samples were separated by a 10% acrylamide gel and electronically transferred to nitrocellulose membrane (Hybond-C, AMERSHAM) at 100 V for 75 min. The membrane was

blocked with PBS containing 10% skimmed milk for 1 h at room temperature before it was incubated with indicated primary and secondary antibodies, respectively. Protein blot bands were detected by the MILLIPORE chemiluminescent HRP substrate kit. The antibodies used in this study were as follows: anti-GFP antibody (JL-8 CLONTECH/No. 1814460 ROCHE, 1:1000), anti-Myc antibody (sc-40 SANTA CRUZ, USA, 1:500), anti-ubiquitin antibody used in Liu et al., 2010, anti-HA antibody (sc-7392AC SANTA CRUZ, 1:500) and goat anti-mouse HRP-conjugated antibody (00001-1 PROTEINTECH, USA, 1:2500).

3. RESULTS AND DISCUSSION

3.1. Physical interactions of SLF with S-RNase and SSK1 proteins in *N. benthamiana*

To examine the relations among SLF, S-RNase and SSK1 factors involved in the S-RNase-based self-incompatibility, we established an *ex vivo* protein expression and reaction system in *N. benthamiana* as described previously (Liu et al., 2010). The *N. benthamiana* protein expression and reaction system has been widely used for protein interaction analysis, protein localization observation and protein ubiquitination and degradation assays (Liu et al., 2010).

First, we determined the optimal conditions for protein expression by agroinfiltration and assessed their protein expression property in the system. We selected the widely used *Agrobacterium* strain EHA105 as a host for our constructs, since it has been shown to be compatible with many binary vectors. Since it is known that different gene constructs could result in largely varied protein expression levels, we examined the expressions of PhS_{3L}RNase-GFP, MYC-PhSLF-S_1, PhSSK1-GFP and MYC-PhSSK1 (Fig. S1) at various time points after inoculation in the presence or absence of p19, a gene-silencing suppressor factor. Non-infiltrated *N. benthamiana* leaves of the wild type was used as a negative control and the sample loading controls were Coomassie brilliant blue staining. In most cases, expressed proteins were almost undetectable after 5 days. We thus used 1, 3 and 5 days after inoculation as sample collection time points. As is shown, for the PhS_{3L}RNase-GFP protein, we found that the 3-day's sample exhibited a relatively higher protein expression level than the 1-day and 5-day's ones, especially with co-infiltration of p19 (Fig. 1A). Thus, an optimal protein expression condition for the PhS_{3L}RNase-GFP protein was determined to be 3-days with p19 factor. For the MYC-PhSLF-S_1 protein, a higher expression level was detected in the 3- and 5-day samples, and the p19 co-infiltration could enhance the protein expression levels especially in the 5-day sample. However, the 1-day sample showed a dramatically low level of the protein expression (Fig. 1B). Thus, 3- and 5-days proved to be the optimal time points for sample collection of the MYC-PhSLF-S_1 protein. The expression of PhSSK1-GFP protein was hardly detectable in 1-day sample, but dramatically increased in the 3-day sample, especially with p19 co-infiltration. However, a reduction of the protein expression was observed at 5-days post-infiltration (Fig. 1C). The optimal protein expression condition was thus similar to that used for the PhS_{3L}RNase-GFP protein. Meanwhile, for the MYC-PhSSK1 protein, an increasing amount of protein production was detected after 3-day of infiltration, and a slightly decrease occurred after 5-day of infiltration. Again, the p19 co-infiltration enhanced the protein expression level (Fig. 1D). In addition, we found that these proteins had a similar expression pattern in *N. benthamiana*, and chose the 3-day with p19 factor co-infiltration as our sample collection time point for the following studies.

Second, a confirmation of their physical interactions in *N. benthamiana* was required for subsequent experiments. As is known, S-RNase interacts with SLF protein, and SSK1 adaptor interacts with SLF *in vitro* and *in vivo* (Qiao et al., 2004a; Huang et al., 2006; Hua et al., 2007; Zhao et al., 2010). We thus examined the interaction between S-RNase and SLF proteins. Two different binary vectors, one carrying a 35S-driven *PhS_{3L}RNase-GFP* expression cassette and the other harboring a 35S-driven *MYC-PhSLF-S_1* expression cassette, were transformed into *A. tumefaciens* EHA105 strain. We collected the leaf samples and extracted proteins for an immunoprecipitation assay. The protein extracts were immunopurified with anti-MYC antibody to pull down the MYC-PhSLF-S_1 proteins, and then the immunoprecipitated products were detected by anti-GFP antibody. The PhS_{3L}RNase-GFP protein could only be pulled down in the mixture of MYC-PhSLF-S_1 and PhS_{3L}RNase-GFP extracts, confirming their interaction (Fig. 1E). To examine the physical interaction between SLF and SSK1 proteins, we co-transformed two constructs carrying a 35S-controlled *MYC-PhSLF-S_1* and a 35S-controlled *PhSSK1-GFP* expression cassette. After the leaf proteins were extracted, we performed the same assay by immunopurifying the sample with anti-GFP antibody and western blot detection with anti-MYC antibody. In this assay, the MYC-PhSLF-S_1 protein could only be detected in the mixture of MYC-PhSLF-S_1 and PhSSK1-GFP extracts, indicating their direct interaction (Fig. 1F). We also excluded the possibility that MYC-SLF protein interacts with a GFP tag protein (Fig. S2). These results confirmed that the physical interactions between SLF-S-RNase and SLF-SSK1 proteins also occur in *N. benthamiana*.

3.2. SLF protein stability is regulated through the ubiquitin−proteasome system in *N. benthamiana*

When we expressed the SLF protein, the SLF protein samples appeared to be modified or bound with other proteins (Fig. 1B). Recent studies have shown that the protein stability of the F-box proteins could be regulated by the ubiquitin−proteasome pathway (Pashkova et al., 2010). To test this idea, we examined whether the SLF protein was associated with ubiquitin. The results of protein blot using anti-MYC antibody revealed that the bands of higher molecular weights were associated with SLF protein fused to MYC tag (Fig. 2A). Next, we used anti-MYC antibody to purify the sample after the extraction of leaf protein, and detected it with anti-Ub antibody. The protein blot analysis using anti-Ub antibody indicated that the bands of higher molecular weights also were

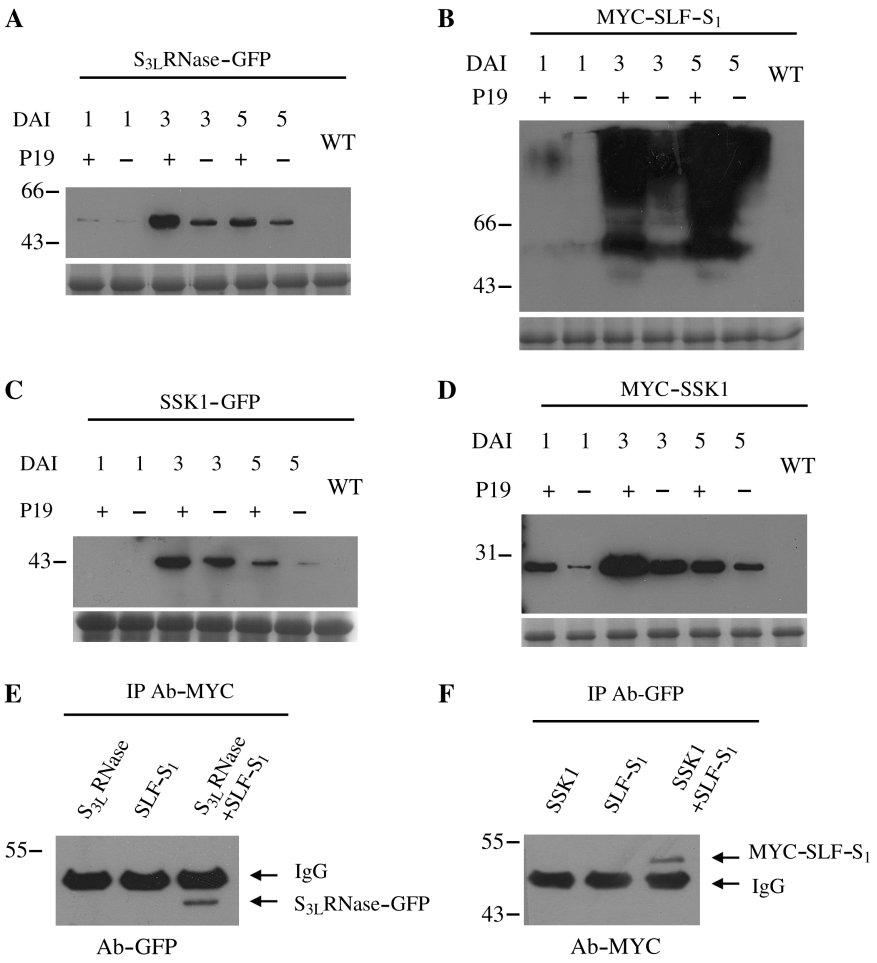

Fig. 1. SLF interacts with both S-RNase and SSK1 in *N. benthamiana*.

A−D: time-course analysis of the expression levels of the four proteins (S_{3L}RNase-GFP, MYC-SLF-S_1, SSK1-GFP and MYC-SSK1) used in this study and the effects of p19 factor on the protein expression in *N. benthamiana*. Leaf was collected on the first, third and fifth day after infiltration. The medium of *Agrobacteria* containing the construct was mixed with (1:1) or without *Agrobacteria* containing p19, respectively, to determine the influence of p19 on the expression outcome of the expressed proteins. WT indicates non-infiltrated *N. benthamiana* leaves used as a negative control. The sample loading controls are Coomassie brilliant blue staining. **E:** S-RNase and SLF interact with each other in *N. benthamiana*. The *Agrobacteria* transformed with the *S_{3L}RNase-GFP* and/or *MYC-SLF-S_1* were infiltrated into healthy leaves of *N. benthamiana* and the leaves collected 3 days after infiltration. The leaf proteins were extracted and incubated with anti-MYC antibody for immunoprecipitation experiments. The samples were detected with anti-GFP antibody by Western blot. The arrows indicate the molecular weight position of IgG band and S_{3L}RNase-GFP protein, respectively. **F:** SLF and SSK1 interact with each other in *N. benthamiana*. The *Agrobacterium* transformed with the *SSK1-GFP* and/or *MYC-SLF-S_1* were infiltrated into healthy leaves of *N. benthamiana* and the leaves collected 3 days after infiltration. The leaf proteins were extracted and incubated with anti-GFP antibody for immunoprecipitation experiments. The samples were detected with anti-MYC antibody by Western blot. The arrows indicate the molecular weight position of IgG band and MYC-SLF-S_1 protein, respectively. The molecular weights are shown on the left of each panel in kDa.

associated with ubiquitin (Fig. 2A). These results led us to further examine the fate of the ubiquitin-associated bands. Since it is widely known that the polyubiquitin-associated proteins are usually targeted to the proteasome system for degradation, we employed a specific inhibitor of 26S proteasome, MG132, to test whether the ubiquitin-associated SLF proteins were degraded by this pathway. We infiltrated MG132 12 h before the leaf samples were harvested and detected the targeted protein as indicated (Fig. 2B). The ubiquitin-associated SLF proteins appeared to accumulate after the treatment of MG132, suggesting that these ubiquitin-associated proteins were recognized and degraded by the 26S proteasome pathway in *N. benthamiana* (Fig. 2B). To ascertain whether the transcriptional level was affected, the expressed target gene and *Actin* mRNA expression levels were analyzed with reverse transcriptase-polymerase chain reaction (RT-PCR), indicating that the transient expression levels of individual genes remained unaltered (Fig. 2B). Therefore, the SLF protein in *N. benthamiana* appeared to be regulated through the ubiquitin−proteasome system.

3.3. SLF interacts with ubiquitin through a putative ubiquitin-binding domain

In most cases, the F-box proteins are reported to bind ubiquitin through a ubiquitin-binding domain structure, such as WD40-repeats or leucine-rich repeats (LRR) domain, which is also present in other non-F-box proteins. Besides, the F-box proteins could also be ubiquitinated in the context of the SCF complex by other SCF complexes or non-SCF E3 complexes.

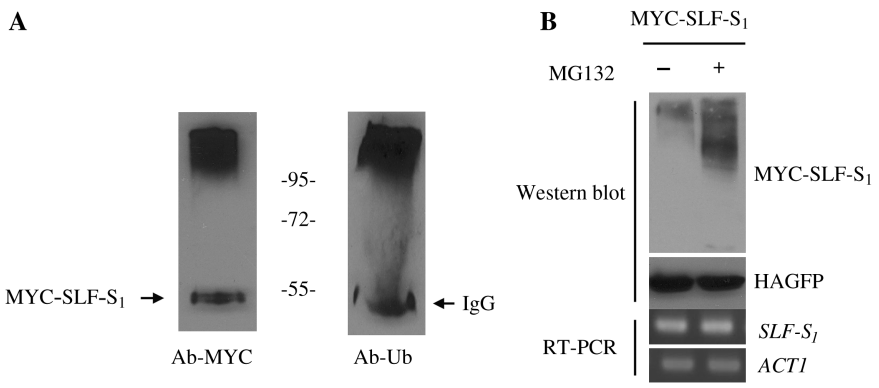

Fig. 2. SLF is autoubiquitinated and degraded through the 26S proteasome pathway in *N. benthamiana*.
A: the *Agrobacteria* transformed with the *MYC-SLF-S_1* were infiltrated into healthy leaves of *N. benthamiana*. After the extraction of leaf proteins, we used an anti-MYC antibody to purify the sample for detection with anti-Ub antibody. The molecular weights are shown between the panels in kDa. **B:** effects of MG132 on the protein stability of SLF in *N. benthamiana*. The *Agrobacteria* transformed with the *MYC-SLF-S_1* were infiltrated into healthy leaves of *N. benthamiana* and the leaves collected 3 days after infiltration. Twelve hours before leaf collection, MG132 was infiltrated into the leaves. The leaf proteins were extracted and detected with anti-MYC and anti-HA antibodies by Western blot, respectively. The total RNA was isolated and reverse transcription performed to obtain cDNA for PCR amplification by specific primers of *SLF-S_1* and *Actin*, respectively.

Thus, we wished to examine whether the SLF proteins have a similar ubiquitin binding property.

To test whether the C-terminal domain (CTD) of SLF protein could bind ubiquitin, we employed the yeast two-hybrid system and made *AD::ubiquitin*, *BD::PhSLF-S_{3L}-C* and *BD::PhSLF-S_1-C* constructs for co-transformation. We performed a quantification assay in the yeast two-hybrid system and found that the SLF proteins could interact with ubiquitin with a similar protein affinity (Fig. 3A).

To examine whether the ubiquitin binding property of the SLF CTD was due to a putative ubiquitin-binding domain, we next generated point-mutated ubiquitin according to previous reports for further interaction test (Pashkova et al., 2010). It is known that for simple ubiquitin-binding domains like UIM (ubiquitin interaction motif), the major binding sites in ubiquitin are defined to be L8, I44 and V70 as a hydrophobic patch (Hofmann and Falquet, 2001; Swanson et al., 2003). Thus accordingly we made the L8A, R42E and I44A mutated ubiquitins and tested their interaction affinity with the CTD of the SLF proteins in the yeast two-hybrid system. It showed that the point-mutations of L8A, R42E and I44A in ubiquitin (Ub*) destroyed its interaction with SLF proteins, suggesting that the SLF protein interacts with ubiquitin through a putative ubiquitin-binding domain in its C-terminal protein−protein interaction region (Fig. 3A).

To confirm the interaction between SLF and ubiquitin proteins, we also performed the protein pull-down assays. The bacterially-produced MBP-PhSLF-S_1 and MBP-SLF-S_{3L} were subjected to pull-down assays with His alone (Ø); or His-fused to wild-type ubiquitin (Ub); or ubiquitin with L8A, R42E and I44A mutations (ub*). Samples were immunoblotted with anti-MBP antibody. The results of the pull-down assay further confirmed the protein interaction property between SLF and ubiquitin (Fig. 3B). However, there is no significant similarity between SLF proteins and other known protein sequences at the amino acid sequence level, although the sequences of SLF proteins themselves are evolutionarily conserved.

To ascribe a potential function of the CTD of SLF proteins, we first analyzed all the available amino acid sequences of SLF protein in the Protein Data Bank, SWISS MODEL and SMART, revealing a similar FBA (F-box associated) domain without other structural or functional annotations. To search for more information about the CTD of SLF proteins, we next performed a structural analysis by using i-Tasser software (http://zhanglab.ccmb.med.umich.edu/I-TASSER/) that could provide a robust meta-threading alignment for identification of template structures and generates a model after iterative simulations (Fig. 3C) (Roy et al., 2010). I-Tasser recognized 2OVR chain B (human Fbw7) as the closest structural homolog among the five ranked models.

To characterize the structural information provided by i-Tasser, we analyzed the Fbw7 and related protein sequences and found it was an F-box protein with a typical WD40-repeats domain. Interestingly, recent findings have also described a novel and conserved function of the WD40-repeats domain in the Fbw7 as well as in many other WD40-repeats containing proteins (Pashkova et al., 2010). It could mediate the ubiquitination and degradation of the protein themselves through a ubiquitin binding property.

To compare the structural similarity between the SLF CTD and Fbw7 WD40-repeats domain, we used the Dali program (http://ekhidna.biocenter.helsinki.fi/dali_server/) (Holm and Rosenstrom, 2010). The Dali identifies that the protein structural similarity between the WD40-repeats domains and PhSLF-CTD showed a *Z*-score at 10.5. In addition, the output of the Dali structural comparison file also included several Kelch-like domain proteins with significant similarities. These results indicated that, although there was no significant similarity between the SLF CTD and other known protein motif at the amino acid sequence level, the C-terminal domains of SLF proteins exhibited a significant similarity with the WD40-repeats domain at a higher structure level (Fig. S3). This analysis provided a structure-based clue for us to study the working mode of SLF

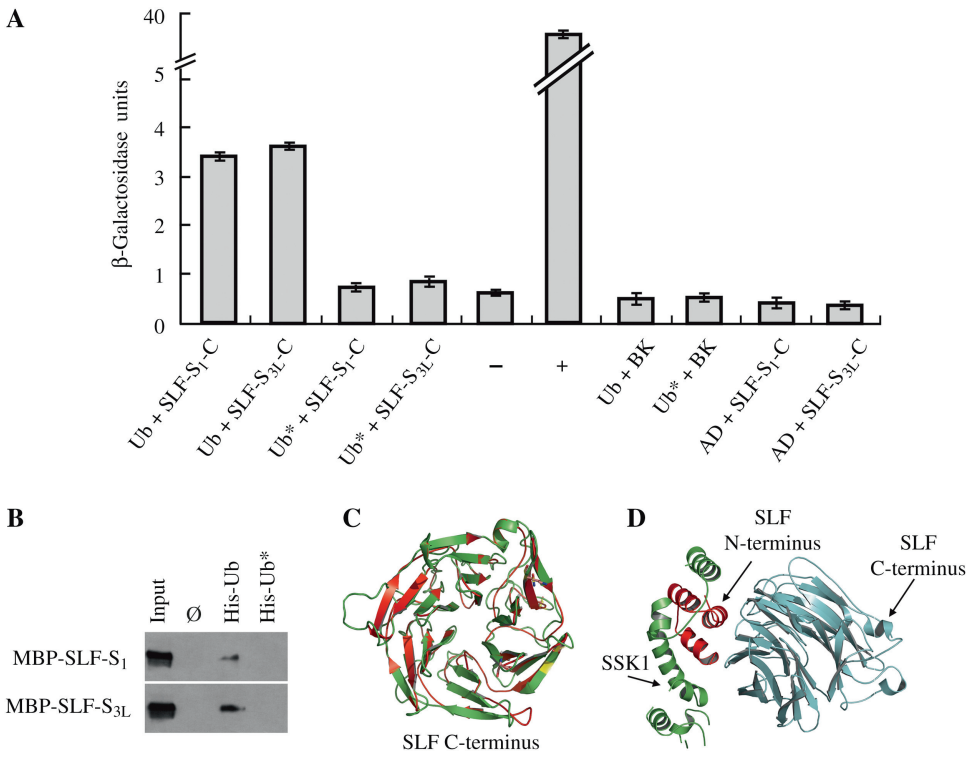

Fig. 3. SLF interacts with ubiquitin through a putative ubiquitin-binding domain.

A: quantitative analysis of protein binding affinity in yeast two-hybrid system. AH109 yeast competent cells were used for co-transformation. "−" and "+" represent the negative and positive experimental controls, respectively. AD-Ub represents the Ub molecule was constructed into AD plasmid, whereas AD-Ub* indicates the ubiquitin with L8A, R42E and I44A mutations constructed into AD plasmid. *PhSLF-S_{3L}-C* and *PhSLF-S_1-C* were constructed into BK plasmid. Self-activation reactions of the four constructs were tested as controls. The quantitative analysis was based on the activity value of the β-galactosidase substrate ONPG reaction. The protein−protein interaction affinity value was normalized according to the following formula: $1000 \times OD_{420}/(t \times V \times OD_{600})$. The X axis indicates the interaction protein pair for detection, whereas the Y axis indicates the normalized activity value of β-galactosidase. **B:** protein pull-down assay of SLF and ubiquitin proteins. The bacterially-expressed MBP-PhSLF-S_1 and MBP-SLF-S_{3L} were subjected to pull-down assays with His alone (Ø); or His-fused to wild-type ubiquitin (Ub); or ubiquitin with L8A, R42E and I44A mutations (ub*). Samples were immunoblotted with anti-MBP antibody. Input lysate sample represents a 10% equivalent. **C:** top view of a predicted three dimensional structure of the C-terminus of SLF protein by I-TASSER. **D:** a predicted three dimensional structure of the SSK1-SLF protein interface. The green helix indicates the conserved SSK1 part, the red helix the conserved N-terminus of SLF part and the blue sheets the C-terminus of SLF structure from a side view.

proteins especially its C-terminal protein−protein interaction domain.

To examine the idea that the SLF proteins have a conserved working mode with SSK1 proteins like other SKP1-F-box proteins, we predicted the SSK1-SLF interface using the ICM-Chemist-Pro (http://www.molsoft.com/chemistpro/index.html), revealing that SSK1 protein interacts with the F-box motif of an SLF protein in a similar manner with those typical SKP1-F-box proteins (Fig. 3D). Thus, SLF proteins could bind to ubiquitin through a putative ubiquitin-binding domain that is conserved throughout the SLF proteins, and subsequently delivered to the proteasome for its degradation. However, as the interactions tested were all obtained in the yeast system, it was still not clear whether this ubiquitin interaction property plays a role in SLF protein function *in vivo*.

3.4. SLF regulates S-RNase protein stability in *N. benthamiana*

To examine whether the ubiquitin-binding affinity of SLF CTD was involved in SLF protein turnover, we utilized the *N. benthamiana* protein reaction system by co-expressing SLF, S-RNase and SSK1. Recent evidence has shown that SLF appears to form an SCF complex to degrade non-self S-RNase (Qiao et al., 2004a; Hua and Kao, 2006). Thus, we mixed the agrobacterium containing the corresponding constructs of *SLF*, *S-RNase* and *SSK1*, as well as the empty vector of *MYC* for an equal volume of the mixture and the *HAGFP* as an internal control. The volume of the *SLF*-containing agrobacterium was increased as the volume of other factors remained the same. After collection of the protein samples, we detected the amount of S-RNase and observed that the protein level of S-RNase significantly decreased (Fig. 4A). To exclude a possible effect from transcriptional regulation, we also examined the expression levels of *S-RNase* and *Actin* mRNA by RT-PCR assay, showing that the transient expression level of individual gene was not influenced (Fig. 4A). These results suggested that SLF regulates S-RNase protein stability in *N. benthamiana*.

To examine the relation of S-RNase degradation and the ubiquitin−proteasome pathway, we also infiltrated MG132 12 h before the leaf samples were harvested and detected the targeted protein as indicated. Consistent with our previous findings (Qiao et al., 2004a), S-RNase proteins were strongly

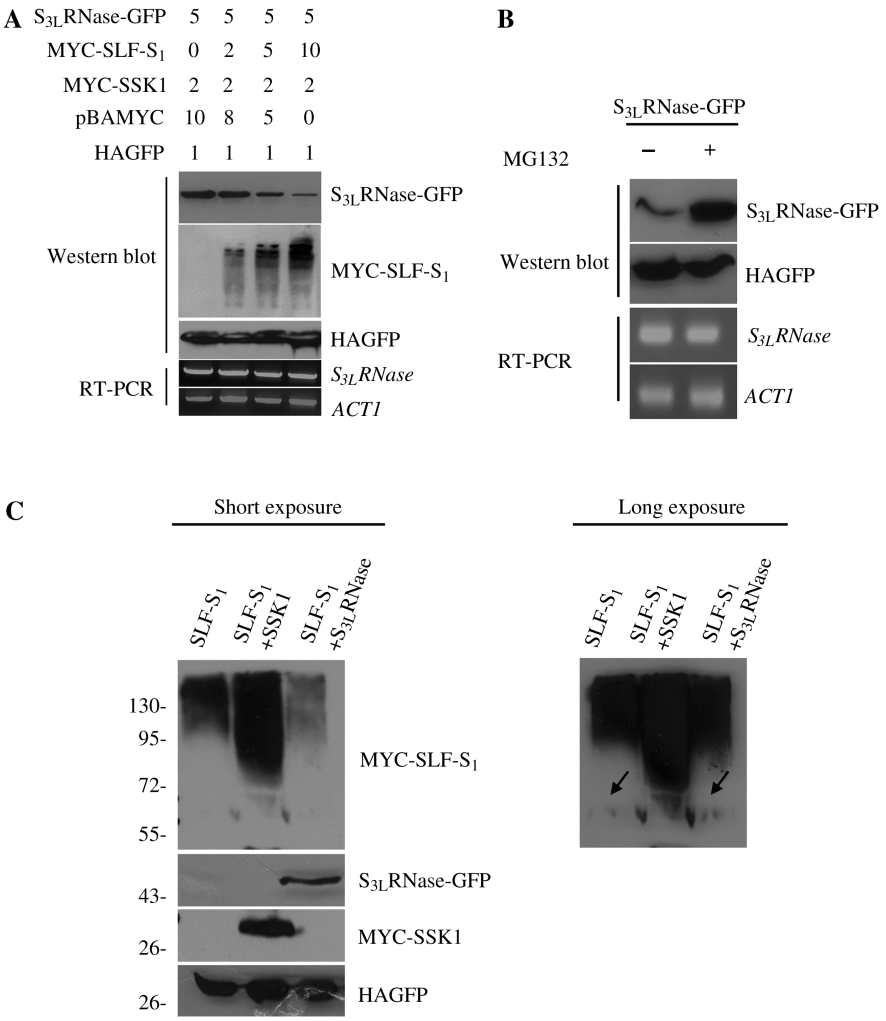

Fig. 4. S-RNase and SSK1 affect SLF protein stability in *N. benthamiana*.

A: SLF targets S-RNase degradation in *N. benthamiana*. The *Agrobacteria* transformed with the *S_{3L}RNase-GFP*, *MYC-SLF-S_1*, *MYC-SSK1*, *pBAMYC* and/or *HAGFP* as indicated were infiltrated into healthy leaves of *N. benthamiana*. The leaves were collected 3 days after infiltration and the leaf proteins and RNA extracted for western blot and RT-PCR analysis, respectively. The first to third panels from top show the Western blot result of the sample by anti-GFP antibody, anti-MYC antibody and anti-HA antibody, respectively; the fourth to fifth panels from top show the RT-PCR results of the sample amplified by primers of *S_{3L}RNase* and *Actin*, respectively. The numbers on the top of the panel indicate the volume of each plasmid-containing *Agrobacteria* in mL. **B:** effects of MG132 on the protein stability of S-RNase in *N. benthamiana*. The *Agrobacteria* transformed with the *S_{3L}RNase-GFP* were infiltrated into healthy leaves of *N. benthamiana* and the leaves collected 3 days after infiltration. Twelve hours before leaf collection, MG132 was infiltrated into the leaves. The leaf proteins were extracted and detected with anti-GFP and anti-HA antibodies by Western blot, respectively. The total RNA was isolated and reverse transcription performed to obtain cDNA for PCR amplification by specific primers of *S_{3L}RNase* and *Actin*, respectively. **C:** effects of S-RNase and SSK1 on SLF protein stability in *N. benthamiana*. The *Agrobacteria* transformed with the *MYC-SLF-S_1* alone or together with the *S_{3L}RNase-GFP* and *MYC-SSK1* were infiltrated into healthy leaves of *N. benthamiana*. After the extraction of leaf protein, the anti-MYC antibody (left, top panel) and the anti-GFP antibody (left, second panel) were used to detect the protein expression level, respectively. HAGFP was used as an internal control for protein loading. The result on the left indicated the X-ray film after a short exposure (30 s), whereas that on the right obtained after a longer exposure (90 s). The arrows indicate the protein molecular weight position of MYC-SLF-S_1.

accumulated after MG132 treatment, showing that S-RNase proteins were degraded by the 26S proteasome pathway in *N. benthamiana* (Fig. 4B). Similarly, to exclude a possible effect of transcriptional level, the expressed target gene and *Actin* mRNA expression levels were also analyzed by RT-PCR experiments, showing that the transient expression level of individual gene was not influenced (Fig. 4B). These results indicated that SLF could target S-RNase for degradation in the proteasome-dependent manner in the *N. benthamiana* system.

3.5. Effects of S-RNase and SSK1 on the SLF protein stability in *N. benthamiana*

To examine possible effects of SSK1 and S-RNase on the SLF protein stability, we co-expressed SLF-SSK1 and SLF-S-RNase proteins, respectively, in *N. benthamiana*. We found that when the SSK1 was co-expressed with SLF proteins, the amount of ubiquitin-binding SLF proteins was significantly increased, indicating that the presence of a specific component of SCF complex promoted the F-box protein instability and

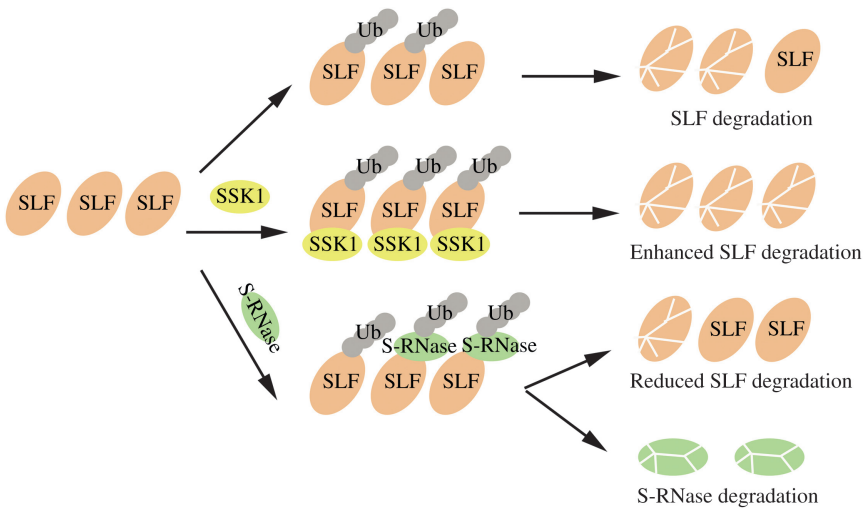

Fig. 5. A model of SLF protein turnover in S-RNase-based self-incompatibility.

a rapid turnover (Fig. 4C). Meanwhile, when we co-expressed the S-RNase with SLF proteins, the protein level of the ubiquitin-binding SLF was reduced dramatically, suggesting that the presence of the specific substrate resulted in F-box protein stability (Fig. 4C). Therefore, we concluded that the protein stability of the SLF proteins is influenced by both SSK1 and S-RNase.

3.6. A model of SLF protein turnover in S-RNase-based self-incompatibility

Our results established that the CTD of SLF protein contains a ubiquitin-binding domain likely involved in its protein turnover. Interestingly, to date, several F-box proteins are found to be UBD-containing proteins (Pashkova et al., 2010). Based on our findings, we propose a model of SLF protein turnover to explain the possible molecular details between SLF-S-RNase recognition. As is shown, three possible states occur during pollination. When SLF is alone, the CTD of SLF would bind ubiquitin and thus recognized by the ubiquitin−proteasome system for its turnover (Fig. 5). When SSK1 is present, SLF autoubiquitination is enhanced and then degraded through the proteasomal pathway (Fig. 5). When S-RNase is present, SLF is stabilized and exhibits reduced autoubiquitination, whereas the S-RNase is ubiquitinated thus degraded through the proteasomal pathway (Fig. 5). In summary, our findings defined a UBD conserved among the SLF with a potential regulatory role in its turnover. Further *in vivo* analysis could help us better understand the SLF function in S-RNase-based self-incompatibility.

ACKNOWLEDGEMENTS

The work was supported by the National Basic Research Program of China (973 Program) (Nos. 2007CB108703 and 2011CB915404) and the National Natural Science Foundation of China (No. 30921003). We gratefully thank Maojun Yang (Tsinghua University, China) for his help of protein structural analysis.

SUPPLEMENTARY DATA

Fig. S1. Schematic representations of the constructs used in the protein expression system of *N. benthamiana*.

Fig. S2. Protein pull-down assay between GFP and MYC-SLF proteins.

Fig. S3. Secondary structural analysis of SLF and Fbw7 proteins.

Table S1. List of primers used in this study.

Supplementary data associated with this article can be found in the online version at doi:10.1016/j.jgg.2012.01.001.

REFERENCES

An, F., Zhao, Q., Ji, Y., Li, W., Jiang, Z., Yu, X., Zhang, C., Han, Y., He, W., Liu, Y., Zhang, S., Ecker, J.R., Guo, H., 2010. Ethylene-induced stabilization of ETHYLENE INSENSITIVE3 and EIN3-LIKE1 is mediated by proteasomal degradation of EIN3 binding F-box 1 and 2 that requires EIN2 in *Arabidopsis*. Plant Cell 22, 2384−2401.

Benkert, P., Tosatto, S.C., Schomburg, D., 2008. QMEAN: a comprehensive scoring function for model quality assessment. Proteins 71, 261−277.

Chen, G., Zhang, B., Zhao, Z., Sui, Z., Zhang, H., Xue, Y., 2010a. 'A life or death decision' for pollen tubes in S-RNase-based self-incompatibility. J. Exp. Bot. 61, 2027−2037.

Chen, V.B., Arendall 3rd, W.B., Headd, J.J., Keedy, D.A., Immormino, R.M., Kapral, G.J., Murray, L.W., Richardson, J.S., Richardson, D.C., 2010b. MolProbity: all-atom structure validation for macromolecular crystallography. Acta Crystallogr. D Biol. Crystallogr. 66, 12−21.

de Nettancourt, D., 2001. Incompatibility and Incongruity in Wild and Cultivated Plants, second ed. Springer, Heidelberg.

Dharmasiri, N., Dharmasiri, S., Estelle, M., 2005. The F-box protein TIR1 is an auxin receptor. Nature 435, 441−445.

Dong, L., Wang, L., Zhang, Y., Deng, X., Xue, Y., 2006. An auxin-inducible F-box protein CEGENDUO negatively regulates auxin-mediated lateral root formation in *Arabidopsis*. Plant Mol. Biol. 60, 599−615.

Finn, R.D., Tate, J., Mistry, J., Coggill, P.C., Sammut, S.J., Hotz, H.R., Ceric, G., Forslund, K., Eddy, S.R., Sonnhammer, E.L., Bateman, A., 2008. The Pfam protein families database. Nucleic Acids Res. 36, D281−D288.

Franklin-Tong, V.E., 2008. Self-Incompatibility in Flowering Plants. Springer, Heidelberg.

Gagne, J.M., Downes, B.P., Shiu, S.H., Durski, A.M., Vierstra, R.D., 2002. The F-box subunit of the SCF E3 complex is encoded by a diverse superfamily of genes in *Arabidopsis*. Proc. Natl. Acad. Sci. USA 99, 11519−11524.

Galan, J.M., Peter, M., 1999. Ubiquitin-dependent degradation of multiple F-box proteins by an autocatalytic mechanism. Proc. Natl. Acad. Sci. USA 96, 9124−9129.

Hofmann, K., Falquet, L., 2001. A ubiquitin-interacting motif conserved in components of the proteasomal and lysosomal protein degradation systems. Trends Biochem. Sci. 26, 347−350.

Holm, L., Rosenstrom, P., 2010. Dali server: conservation mapping in 3D. Nucleic Acids Res. 38, W545−W549.

Hua, Z., Vierstra, R.D., 2011. The cullin-RING ubiquitin-protein ligases. Annu. Rev. Plant Biol. 62, 299−334.

Hua, Z.H., Kao, T.-H., 2006. Identification and characterization of components of a putative *Petunia S*-locus F-box-containing E3 ligase complex involved in S-RNase-based self-incompatibility. Plant Cell 18, 2531−2553.

Hua, Z.H., Meng, X., Kao, T.-H., 2007. Comparison of *Petunia inflata S*-Locus F-Box Protein (Pi SLF) with Pi SLF like proteins reveals its unique function in S-RNase based self-incompatibility. Plant Cell 19, 3593−3609.

Hua, Z.H., Fields, A., Kao, T.-H., 2008. Biochemical models for S-RNase-based self-incompatibility. Mol. Plant 1, 575−585.

Huang, J., Zhao, L., Yang, Q., Xue, Y., 2006. AhSSK1, a novel SKP1-like protein that interacts with the *S*-locus F-box protein SLF. Plant J. 46, 780−793.

Kao, T.-H., Tsukamoto, T., 2004. The molecular and genetic bases of S-RNase-based self-incompatibility. Plant Cell 16 (Suppl.), S72−S83.

Kepinski, S., Leyser, O., 2005. The *Arabidopsis* F-box protein TIR1 is an auxin receptor. Nature 435, 446−451.

Kim, W.Y., Fujiwara, S., Suh, S.S., Kim, J., Kim, Y., Han, L., David, K., Putterill, J., Nam, H.G., Somers, D.E., 2007. ZEITLUPE is a circadian photoreceptor stabilized by GIGANTEA in blue light. Nature 449, 356−360.

Kubo, K., Entani, T., Takara, A., Wang, N., Fields, A.M., Hua, Z., Toyoda, M., Kawashima, S., Ando, T., Isogai, A., Kao, T.H., Takayama, S., 2010. Collaborative non-self recognition system in S-RNase-based self-incompatibility. Science 330, 796−799.

Lai, Z., Ma, W., Han, B., Liang, L., Zhang, Y., Hong, G., Xue, Y., 2002. An F-box gene linked to the self-incompatibility (*S*) locus of *Antirrhinum* is expressed specifically in pollen and tapetum. Plant Mol. Biol. 50, 29−42.

Lee, H.S., Huang, S., Kao, T.-H., 1994. S proteins control rejection of incompatible pollen in *Petunia inflata*. Nature 367, 560−563.

Li, Y., Gazdoiu, S., Pan, Z.Q., Fuchs, S.Y., 2004. Stability of homologue of Slimb F-box protein is regulated by availability of its substrate. J. Biol. Chem. 279, 11074−11080.

Liu, L., Zhang, Y., Tang, S., Zhao, Q., Zhang, Z., Zhang, H., Dong, L., Guo, H., Xie, Q., 2010. An efficient system to detect protein ubiquitination by agroinfiltration in *Nicotiana benthamiana*. Plant J. 61, 893−903.

Mathias, N., Johnson, S., Byers, B., Goebl, M., 1999. The abundance of cell cycle regulatory protein Cdc4p is controlled by interactions between its F box and Skp1p. Mol. Cell Biol. 19, 1759−1767.

McClure, B.A., Gray, J.E., Anderson, M.A., Clarke, A.E., 1990. Self-incompatibility in *Nicotiana alata* involves degradation of pollen rRNA. Nature 347, 757−760.

Murfett, J., Atherton, T.L., Mou, B., Gasser, C.S., McClure, B.A., 1994. *S-RNase* expressed in transgenic *Nicotiana* causes *S*-allele-specific pollen rejection. Nature 367, 563−566.

Nibau, C., Gibbs, D.J., Bunting, K.A., Moody, L.A., Smiles, E.J., Tubby, J.A., Bradshaw, S.J., Coates, J.C., 2011. ARABIDILLO proteins have a novel and conserved domain structure important for the regulation of their stability. Plant Mol. Biol. 75, 77−92.

Pashkova, N., Gakhar, L., Winistorfer, S.C., Yu, L., Ramaswamy, S., Piper, R.C., 2010. WD40 repeat propellers define a ubiquitin-binding domain that regulates turnover of F box proteins. Mol. Cell 40, 433−443.

Patton, E.E., Willems, A.R., Tyers, M., 1998. Combinatorial control in ubiquitin-dependent proteolysis: don't Skp the F-box hypothesis. Trends Genet. 14, 236−243.

Petroski, M.D., Deshaies, R.J., 2005. Function and regulation of cullin-RING ubiquitin ligases. Nat. Rev. Mol. Cell Biol. 6, 9−20.

Qiao, H., Wang, H., Zhao, L., Zhou, J., Huang, J., Zhang, Y., Xue, Y., 2004a. The F-box protein AhSLF-S_2 physically interacts with S-RNases that may be inhibited by the ubiquitin/26S proteasome pathway of protein degradation during compatible pollination in *Antirrhinum*. Plant Cell 16, 582−595.

Qiao, H., Wang, F., Zhao, L., Zhou, J., Lai, Z., Zhang, Y., Robbins, T.P., Xue, Y., 2004b. The F-box protein AhSLF-S_2 controls the pollen function of S-RNase-based self-incompatibility. Plant Cell 16, 2307−2322.

Roy, A., Kucukural, A., Zhang, Y., 2010. I-TASSER: a unified platform for automated protein structure and function prediction. Nat. Protoc. 5, 725−738.

Schulman, B.A., Carrano, A.C., Jeffrey, P.D., Bowen, Z., Kinnucan, E.R., Finnin, M.S., Elledge, S.J., Harper, J.W., Pagano, M., Pavletich, N.P., 2000. Insights into SCF ubiquitin ligases from the structure of the Skp1−Skp2 complex. Nature 408, 381−386.

Sijacic, P., Wang, X., Skirpan, A.L., Wang, Y., Dowd, P.E., McCubbin, A.G., Huang, S., Kao, T.-H., 2004. Identification of the pollen determinant of S-RNase-mediated self-incompatibility. Nature 429, 302−305.

Stuttmann, J., Lechner, E., Guerois, R., Parker, J.E., Nussaume, L., Genschik, P., Noel, L.D., 2009. COP9 signalosome- and 26S proteasome-dependent regulation of SCFTIR1 accumulation in *Arabidopsis*. J. Biol. Chem. 284, 7920−7930.

Swanson, K.A., Kang, R.S., Stamenova, S.D., Hicke, L., Radhakrishnan, I., 2003. Solution structure of Vps27 UIM-ubiquitin complex important for endosomal sorting and receptor downregulation. EMBO J. 22, 4597−4606.

Takayama, S., Isogai, A., 2005. Self-incompatibility in plants. Annu. Rev. Plant Biol. 56, 467−489.

van den Burg, H.A., Tsitsigiannis, D.I., Rowland, O., Lo, J., Rallapalli, G., Maclean, D., Takken, F.L., Jones, J.D., 2008. The F-box protein ACRE189/ACIF1 regulates cell death and defense responses activated during pathogen recognition in tobacco and tomato. Plant Cell 20, 697−719.

Vierstra, R.D., 2009. The ubiquitin-26S proteasome system at the nexus of plant biology. Nat. Rev. Mol. Cell Biol. 10, 385−397.

Wirbelauer, C., Sutterluty, H., Blondel, M., Gstaiger, M., Peter, M., Reymond, F., Krek, W., 2000. The F-box protein Skp2 is a ubiquitylation target of a Cul1-based core ubiquitin ligase complex: evidence for a role of Cul1 in the suppression of Skp2 expression in quiescent fibroblasts. EMBO J. 19, 5362−5375.

Xie, D.X., Feys, B.F., James, S., Nieto-Rostro, M., Turner, J.G., 1998. COI1: an *Arabidopsis* gene required for jasmonate-regulated defense and fertility. Science 280, 1091−1094.

Yan, J., Zhang, C., Gu, M., Bai, Z., Zhang, W., Qi, T., Cheng, Z., Peng, W., Luo, H., Nan, F., Wang, Z., Xie, D., 2009. The *Arabidopsis* CORONATINE INSENSITIVE1 protein is a jasmonate receptor. Plant Cell 21, 2220−2236.

Zhang, Y., Xu, W., Li, Z., Deng, X.W., Wu, W., Xue, Y., 2008. F-box protein DOR functions as a novel inhibitory factor for abscisic acid-induced stomatal closure under drought stress in *Arabidopsis*. Plant Physiol. 148, 2121−2133.

Zhang, Y., Xue, Y., 2008. Molecular biology of S-RNase-based self-incompatibility. In: Franklin-Tong, V.E. (Ed.), Self-Incompatibility in Flowering Plants - Evolution, Diversity and Mechanisms. Springer, pp. 193−215.

Zhang, Y., Zhao, Z., Xue, Y., 2009. Roles of proteolysis in plant self-incompatibility. Annu. Rev. Plant Biol. 60, 21−42.

Zhao, L., Huang, J., Zhao, Z., Li, Q., Sims, T.L., Xue, Y., 2010. The Skp1-like protein SSK1 is required for cross-pollen compatibility in S-RNase-based self-incompatibility. Plant J. 62, 52−63.

Zhou, P., Howley, P.M., 1998. Ubiquitination and degradation of the substrate recognition subunits of SCF ubiquitin-protein ligases. Mol. Cell 2, 571−580.